Reliability Improvement of Large Area Soldering Connections by Antimony Containing Lead-Free Solder

[1]H. Beyer, [1]V. Sivasubramaniam, [1]D. Hajas, [1]E. Nanser, [2]F. Brem

[1]ABB Switzerland Ltd., Semiconductors, harald.beyer@ch.abb.com
[2]ABB Switzerland Ltd., Corporate Research, franziska.brem@ch.abb.com

Abstract

Power semiconductor modules typically undergo extreme thermal excursions, which require reliable large area solder connections. Here antimony (Sb) containing lead-free solders are promising candidates providing very good thermo-mechanical properties. In this work mechanical and microstructural investigations of soldering connections between Ni(P) plated AlSiC baseplates and ceramic substrates using lead-free solders Sn5Sb and Sn8Sb are presented. The metallization for the ceramic substrates were bare copper and NiAu coated copper metallization. Overall results of antimony containing lead-free solders are compared with baseline solders - 62Sn36Pb2Ag and lead-free Sn-Ag-Cu (SAC) solders. The antimony containing lead-free solders exhibit significantly higher shear strength and ductility at ‘as soldered’ condition compared to the baseline solders. After subsequent isothermal aging at high temperature, antimony containing lead-free solders maintain their superior shear strength with good ductility. The sustainance of shear strength and ductility even after high temperature aging suggests, that the reliability of Sn-Sb solders is superior over 62Sn36Pb2Ag and lead-free Sn-Ag-Cu (SAC) solders.

1. Introduction

Due to worldwide environmental regulations like the ‘Restriction of Hazardous Substances’ (RoHS) of the European Union, dangerous and harmful substances are banned from electronic products. Suppliers of power electronic devices are forced to replace commonly used lead containing solders like 62Sn36Pb2Ag by lead-free solders in most applications. Hence, many suppliers introduced lead-free solders like Sn3.5Ag or Sn-Ag-Cu (SAC) solders like SAC305 (96.5Sn3.0Ag0.5Cu) or SAC387 (95.5Sn3.8Ag0.7Cu) having a melting point around 220°C. However, these solders have the disadvantage of poor wetting behavior and low ductility resulting in a reduced reliability of soldering connections against thermo-mechanical stress. The homologous temperatures especially of low melting SnPbAg solders are high. Hence, these solders, but also Sn-Ag or Sn-Ag-Cu based solders are prone to microstructural coarsening, that results in poor high temperature reliability [1].

Lead-free tin-antimony (Sn-Sb) solders seem to be promising candidates to overcome these problems because of their good mechanical properties like creeping behavior [2,3]. The tensile strength of the solder was enhanced with an increasing antimony content related to an improved solid solution strengthening, when alloying tin grains with antimony [4]. The superior reliability of soldering connections using tin-antimony solders against thermo-mechanical stress in comparison to Sn-Ag or Sn-Ag-Cu based solders was shown between chip and substrate [5], but also between substrate and copper baseplate [6] as used in IGBT modules. A strongly suppressed deterioration of Sn-Sb based solder in comparison to Sn-Ag based solder was observed when storing the solders at high temperature. Further, an increasing antimony content in Sn-Sb based solders resulted in an enhancement of the thermal cycling reliability of large area solder joints [4,7]. Finally, Sn-Sb based solders provide economic advantages due to their competitive price in comparison to SnPbAg, SnAg, or SAC solders.

Despite the reported improvement in thermal reliability of Sn-Sb solders, there are barely a few IGBT module producers utilizing lead-free solders for substrate soldering. This work is therefore focused to systematically understand the property improvement in Sn-Sb solders by correlating their mechanical properties to the microstructural evolution during high temperature isothermal aging.

In this work, shear tests and microstructural analysis of soldering connections between Ni(P) plated AlSiC baseplates and ceramic substrates with bare and NiAu coated copper metallization using the antimony containing lead-free solders Sn5Sb and Sn8Sb are presented. The results from 'as soldered' and isothermally aged samples are compared to 62Sn36Pb2Ag solder and lead-free SAC solders.

2. Experimental

2.1. Sample Preparation

Samples were prepared by soldering ceramic substrates with a size of about 50 x 50 mm^2 having bare (1.0 mm AlN ceramic thickness) and NiAu coated copper metallization (0.63 mm Si_3N_4 ceramic thickness), respectively, to Ni(P) plated AlSiC baseplates. The substrates were soldered using solder preforms in a single chamber vacuum soldering furnace with formic acid gas. Nominal soldering temperatures (machine settings) of 295-315°C were used for Sn5Sb solder ($T_{liquidus}$ = 240°C) and of 305-325°C for Sn8Sb ($T_{liquidus}$ = 246°C). Reference samples with lead containing solder 62Sn36Pb2Ag (SnPbAg) and lead-free 96.5Sn3.5Ag0.5Cu (SAC305) and 95.5Sn3.8Ag0.7Cu (SAC387) were also prepared. Isothermal aging of soldered connections was performed in an oven at 170°C for 1,000 hours.

Samples for metallographic cross sections and shear tests were prepared from soldered substrate-baseplate assembly by water jet cutting, which is reported to cause less artefacts of the cross-sectional areas in comparison to traditional cutting by diamond saw [8]. Here the CNC based process of water jet cutting provides a high dimensional reproducibility of the samples for shear tests having a nominal size of 10x10 mm^2. Metallographic cross sections underwent a classical polishing procedure with a final polishing using oxide polishing suspension (OPS, 50 nm SiO_2 particles) and etching step to reveal the Sn grains with 5% HCl.

2.2. Sample Characterization

Void inspection of the soldering connections was done by scanning acoustic microscope (SAM). The metallographic specimen were analyzed by light microscope and SEM/EDX with focus on the formation of intermetallic phases on the bulk and at interfaces between solder and substrate/baseplate metallization, respectively. The cross-sections were investigated only at 'as soldered' and at aged condition for 1,000 hours at 170°C.

The mechanical strength of the soldering connections was determined by shear tests in a standard tension tester with a cross-head speed of 20 mm/min. In addition to the shear strength, the shear distance related to the ductility was determined from the peak width of the force-distance curve at 1,000 N. A large peak width is related to a ductile behavior and a small peak width to a more brittle behavior of the soldering connection. For evaluation, the mean values of shear strength and shear distance based on 5–14 samples were calculated with error bars representing 95% confidence level of the mean value.

Finally, the fracture behavior (ductile/brittle) in the shear test was determined by visual observation and SEM. It was categorized as cohesive fracture (shearing through bulk solder) or as adhesive fracture (breaking on interfaces between solder and joining partners).

3. Results

3.1. Shear Tests

Shear Strength

Figure 1 shows the average shear strength of ‘as soldered’ and aged samples of both metallization types for different nominal soldering temperatures in comparison to SnPbAg solder and SAC solders. For ‘as soldered’ conditions, higher shear strength was measured for substrates with bare copper metallization for all samples under consideration, but accompanied with larger error bars except for SnPbAg solder. Significantly highest shear strength was measured for samples soldered with Sn8Sb compared with Sn5Sb and baseline solders. With bare Cu metallization, Sn5Sb showed an average shear strength of approximately 83 MPa, and for Sn8Sb up to 91 MPa were measured. For substrates with NiAu metallization, the average shear strength was 72 MPa for Sn5Sb and 81 MPa for Sn8Sb. For SnPbAg solder, the average shear strength was 65 MPa, whereas SAC solders achieved a shear strength of 70 MPa for substrates with bare copper metallization and 59 MPa for substrates with NiAu coating. No significant influence of soldering peak temperature on the shear strength was observed for antimony containing solders.

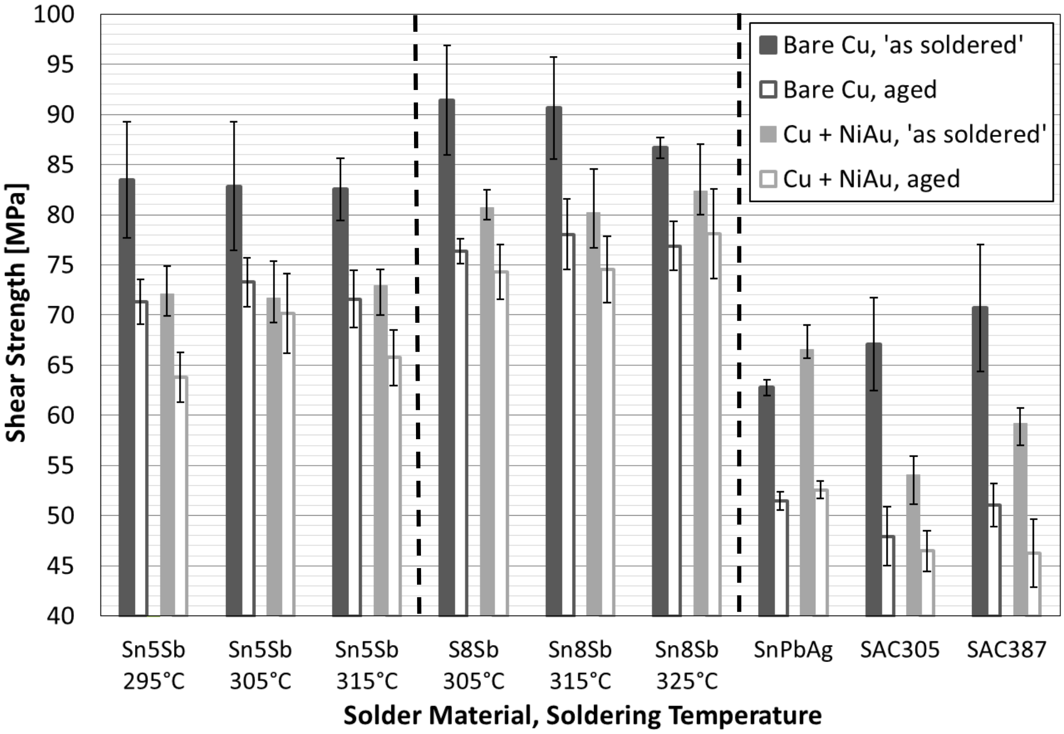

Fig. 1. Average shear strength of ‘as soldered’ and aged soldering connections of substrates with bare and NiAu coated copper metallization prepared by Sn5Sb and Sn8Sb compared with soldering connections using SnPbAg and SAC solders.

For the aged condition, all the solder samples and metallization types exhibited a reduction of shear strength compared with ‘as soldered’ samples. However after aging, samples soldered with Sn-Sb based solder showed significantly higher shear strengths than baseline solders. With bare Cu metallization, samples soldered with Sn5Sb had an average shear strength of 71 MPa, and with Sn8Sb the shear strength was 76 MPa. This corresponds to a decrease of shear strength of up to 15 MPa from its ‘as soldered’ shear strength values. For substrates with NiAu metallization, the shear strength typically decreased by 8 MPa with shear strength of 64-70 MPa for Sn5Sb and approximately 75 MPa for Sn8Sb. Even with the variation in substrate metallization, the shear strength of aged Sn-Sb solders remained significantly higher than base-line solders’ shear strength.

Ductility

The ductility of a soldering connection is related to the shear distance shown by the peak width of the measured force-distance curve. Figure 2 shows average shear distances. For ‘as soldered’ samples, the largest shear distance of up to 1.05 mm was determined for Sn-Sb solders. However, slightly lower shear distance was observed for Sn8Sb compared to Sn5Sb. A decrease of the shear distance with increasing soldering temperature was observed for substrates with bare copper metallization, whereas no significant change in the shear distance was observed for NiAu coated substrates. Significantly smaller shear distances of approximately 0.8 mm were determined for SnPbAg and both SAC solders.

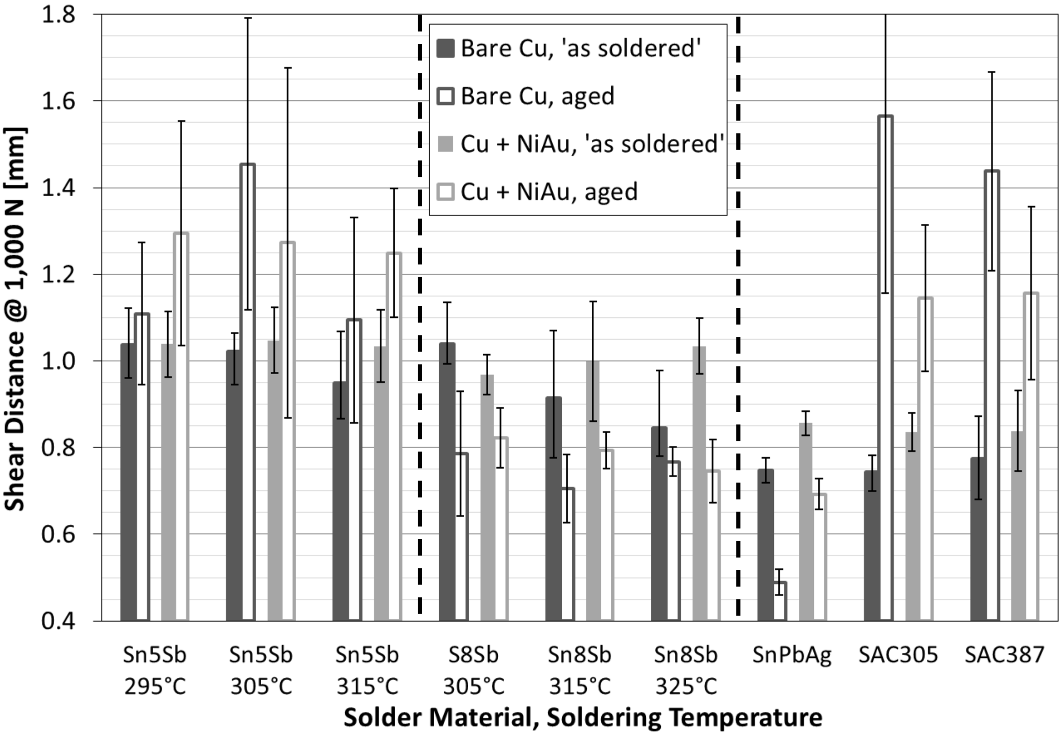

Fig. 2. Average shear distance of ‘as soldered’ and aged soldering connections on substrates with bare and NiAu coated copper metallization prepared by Sn5Sb and Sn8Sb compared with soldering connections of SnPbAg and SAC solders.

After aging, highest shear distances were observed for samples soldered with Sn5Sb and both SAC solders, exceeding their respective values for ‘as soldered’ condition. Samples soldered with Sn5Sb exhibited shear distances between 1.1 mm and 1.45 mm for substrates with bare copper metallization and up to 1.3 mm for NiAu coated substrates. Samples soldered with SAC solders had an average shear distance of 1.55 mm for substrates with bare copper metallization and 1.15 mm for NiAu coated substrates. A reduced shear distance indicating reduced ductility was observed on samples soldered with Sn8Sb and SnPbAg solder. Significantly smaller shear distance between 0.7 mm and 0.85 mm was determined for samples soldered with Sn8Sb solder for both substrate metallizations. For samples soldered with SnPbAg solder, between 0.5 mm and 0.7 mm were determined for both metallizations types.

Fracture Behavior

For ‘as soldered’ samples, mostly adhesive fracture was observed on substrates with bare copper metallization for all solders, where crack propagation was predominantly observed at the interface between solder and joining partners. Cohesive fracture was observed only on a few samples with Sn5Sb or SnPbAg solder. Mostly cohesive fracture was observed on NiAu coated substrates soldered with antimony containing solders, whereas the occurrence of adhesive fracture increased typically at higher process temperature. After aging, samples soldered with Sn5Sb and SAC solder mostly showed cohesive fracture behavior, which is an indicator for ductile behavior. Samples prepared with Sn8Sb solder and SnPbAg solder showed more adhesive fracture behavior, which is an indicator for brittleness.

Figure 3 shows SEM pictures taken in SE (secondary electron) mode of fracture surfaces of substrates with bare copper metallization soldered with Sn5Sb (a) and Sn8Sb (b) after aging. The fractograph for the soldering connection prepared by Sn5Sb shows typical shear bands indicating a ductile cohesive fracture in the bulk solder. For Sn8Sb, the fractograph shows a typical brittle adhesive fracture behavior. Large particles are (CuSnNi)(Sb) intermetallics.

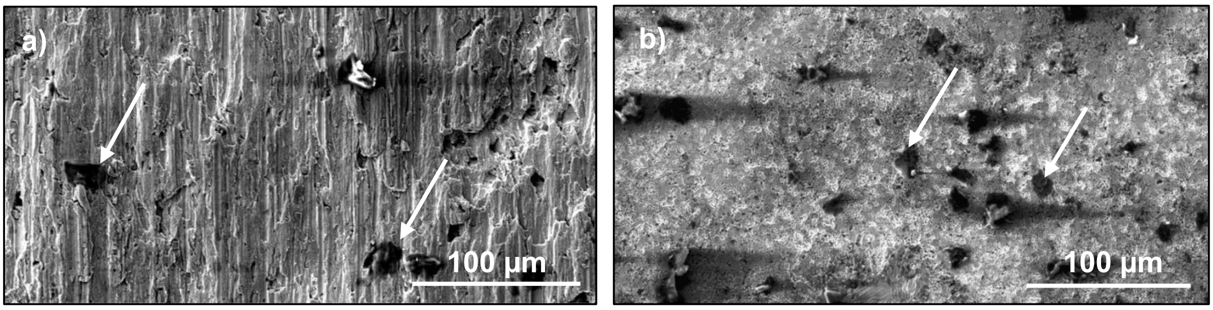

Fig. 3. Fractographs recorded in SE mode of soldering connections prepared by Sn5Sb (a) and Sn8Sb (b) after aging. Arrows show particles of (CuSnNi)(Sb) intermetallics.

3.2. Microstructural Analysis

Figure 4 shows a micrograph (500x magnification) of bulk solder prepared with Sn5Sb solder for a substrate with bare copper metallization. The micrograph shows a typical microstructure of an aged sample, where the microstructure was constituted with β-Sn islands with its grain boundaries decorated with a fine homogeneous distribution of Sn-Sb intermetallic particles.

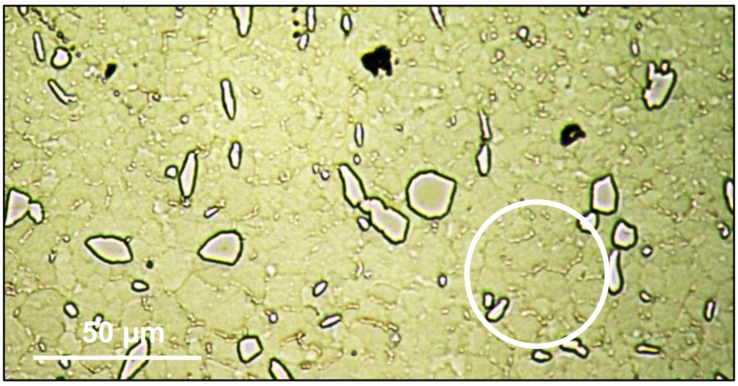

Fig. 4. Micrograph (500x) of bulk Sn5Sb solder (aged condition) of a soldering connection prepared with bare copper metallization. β-Sn grains surrounded with fine particles of Sn-Sb intermetallic phase are encircled for better understanding.

Figure 5 shows micrographs (500x magnification) of soldering connections prepared by Sn5Sb on both investigated substrate metallization types. Intermetallic phases are shown from the substrate-solder interface, and from the baseplate-solder interface. For ‘as soldered’ condition, a thin Cu_3Sn phase and a (CuSnNi) phase with antimony in solid solution was formed on the interface between copper and solder for substrates with bare copper metallization. A large amount of precipitations was observed in the bulk solder. The antimony content matched well with the weight% of antimony in the solder. At the interface between solder and baseplate a (CuSnNi)(Sb) phase was observed. The weight% of copper and tin matched to the well reported Cu_6Sn_5 intermetallic phase. For NiAu coated metallized substrates soldered to baseplates with Ni(P) surface layer, on both sides a formation of the intermetallic Ni_3Sn_4-phase was observed with antimony in solid solution. No precipitations in the bulk solder were observed. Both intermetallic phases were looking less dense in comparison to samples with bare copper metallized substrate. Similar phase formation behavior was observed for Sn8Sb solder.

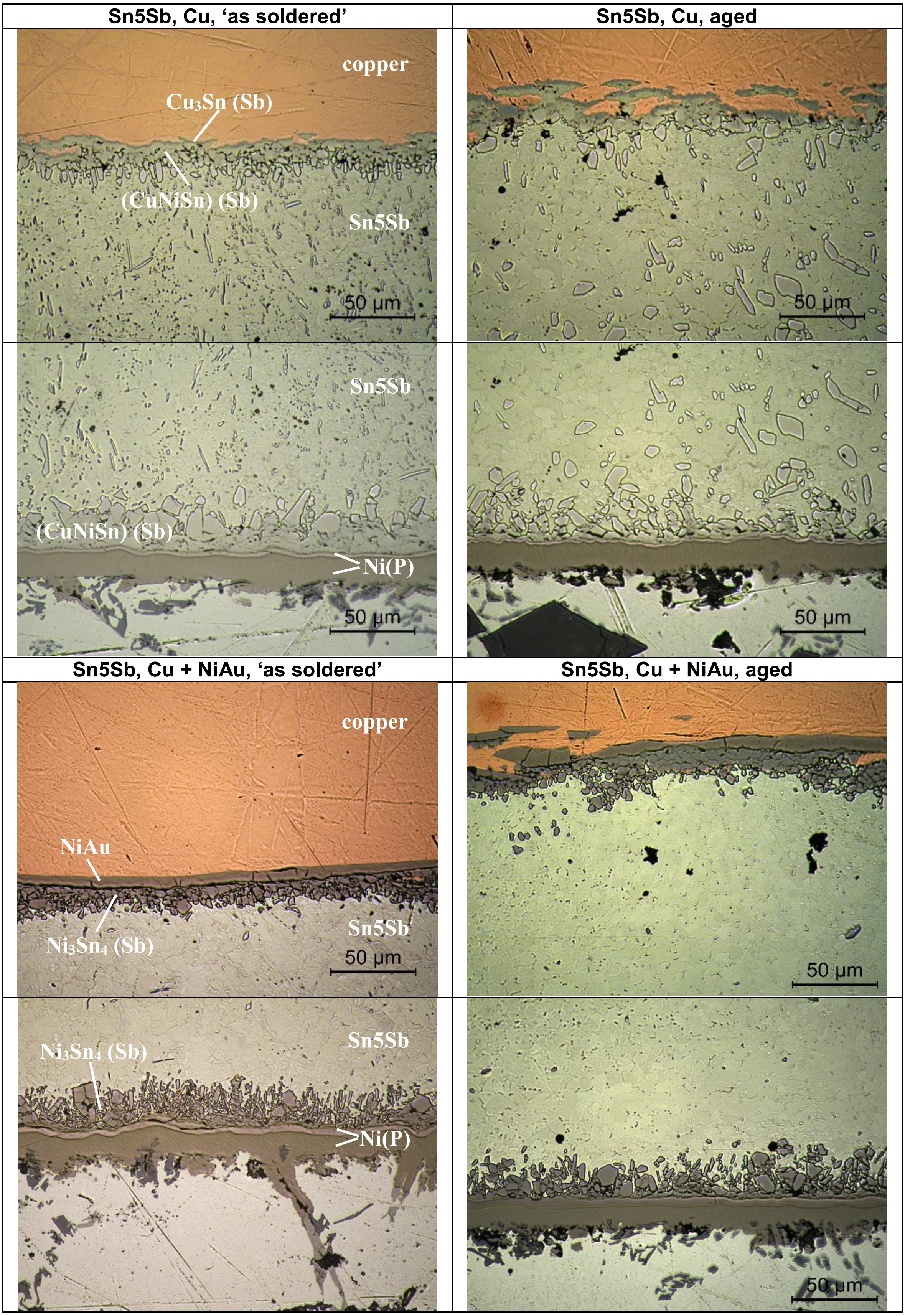

Fig. 5. Optical micrographs of ‘as soldered’ and aged samples with Sn5Sb solder.

After aging, for bare copper metallized substrates, there were bigger interfacial intermetallic (CuNiSn)(Sb) particles (10-50 µm) visible in bulk solder, see figure 4. It is hypothesized, that during soldering some of the formed interfacial intermetallics could have spalled into the bulk solder. Possible reasons are longer soldering times and crystal structure mismatch between various intermetallics under consideration [9]. The precipitations observed in bulk solder on 'as soldered' substrates with bare copper metallization have diffused to the interfaces to form larger (CuSnSb) intermetallics. For NiAu metallized substrates, the (SnSb) intermetallic did not show significant growth. However for both metallization types, the morphology of the β-Sn grains surrounded by finer (SnSb) intermetallic was quite stable in size and morphology even after isothermal thermal aging.

For the aged condition, the intermetallic phases on the substrate-solder interface were more compact and evolved into more homogenously thick layer for both substrate types compared with 'as soldered' condition. It was observed, that multiple smaller intermetallic phases at the interface grow into denser chunks. These constituted to a denser and thicker intermetallic on the interface. A similar trend in the microstructure was also observed with Sn8Sb. However, an increase in the volume fraction of the (SnSb) intermetallic phases was observed with larger needle like morphology for (SnSb) intermetallic in the bulk solder.

4. Discussion

The results of shear tests on 'as soldered' samples show significantly enhanced shear strength and ductility for Sb containing solders in comparison to SAC or SnPbAg solders. In general, for both Sn-Sb solders, the shear strength was higher for substrates with bare copper metallization compared to substrates with NiAu coated metallization. One possible explanation may be the formation of (SnSb) precipitations in the bulk solder for bare copper metallization strengthening the soldering connection. This was not observed on the substrates with NiAu coating.

After aging, the decrease of shear strength for substrates with bare copper metallization was significantly higher than for substrates with NiAu coated metallization accompanied by a transition from brittle adhesive to ductile cohesive fracture behavior for Sn5Sb. This loss of shear strength may be attributed to the diffusion of finer (SnSb) precipitations from the bulk solder to the interfaces forming larger (CuNiSn)(Sb) intermetallics. Bare Cu metallization is capable of promoting (CuNiSn)(Sb) intermetallic phase growth in the bulk solder that could have affected also the ductility after isothermal aging.

Sn8Sb provided higher shear strength than Sn5Sb, but accompanied with limited ductility. The high shear strength of Sn8Sb may be attributed to higher volume fraction of the (SnSb) grains that may on one hand help reinforcing the solder matrix for higher strength, but on the other hand act as stress localization sights, leading to a reduced ductility compared to Sn5Sb. This is consistent with results from literature showing, that an increase in Sb content allows higher strength because of solid solution strengthening effect [4,7]. The Sn5Sb showed a superior ductility, which may be attributed to the finer (SnSb) grains around the β-Sn islands. Further, with NiAu metallization, Ni is hypothesized to have functioned as a diffusion barrier that helps preserving the fine (SnSb) microstructure by restricting the Cu diffusing from substrate into bulk solder. This could be attributed as a reason for the stability of finer (SnSb) grains around β-Sn even after aging.

5. Conclusion and Outlook

Mechanical and microstructural investigations were performed on soldering connections between substrates having bare and NiAu coated copper metallization and Ni(P) coated AlSiC baseplates prepared by antimony containing lead-free solders Sn5Sb and Sn8Sb in comparison to soldering connections prepared by SnPbAg and SAC solders.

On one hand Sn-Sb solder offered the highest shear strength and ductility on ‘as soldered’ samples for both metallization types. Upon aging, Sn-Sb solders exhibited significantly improved properties with respect to shear strength accompanied by good ductility solder after high temperature aging against the baseline solders. This was reflected in a minimal reduction of shear strength even after aging in comparison to SnPbAg and SAC solders. Approximately, Sn-Sb solders maintained about 50% higher shear strength after thermal aging compared with SnPbAg and SAC solders.

One has to consider carefully according to the application the Sb content in the solder. It was demonstrated with Sn5Sb showing good shear strength with superior ductility suited for connections having large CTE mismatch (e.g. Cu baseplates with Al_2O_3 substrate). On the other hand Sn8Sb showed the highest shear strength with acceptable ductility to suit more to AlSiC baseplates with AlN or Si_3N_4 substrates with lower CTE mismatch. Beside of these clear improvements of shear strength and ductility of Sn-Sb solders, further improvement related to specific applications may be possible by alloying with minute additives e.g. by germanium, bismuth or silver [10].

6. Literature

[1] Morozumi, A; Yamada, K.; Miyasaka, T.; Sumi, S.; Seki, Y.: Reliability of Power Cycling for IGBT Power Semiconductor Modules. IEEE Transactions on Industry Applications Vol. 39-3 (2003), pp. 665-671.

[2] Mahmudi, R.; Geranmayeh, A.R.; Bakherad, M.: Indentation creep study of lead-free Sn-5%Sb solder alloy. Materials Science and Engineering A Vol. 457 (2007), pp.173-179.

[3] Mahmudi, R.; Geranmayeh, A.R.; Razaee-Bazzaz, A.: Impression creep behavior of lead-free Sn-5Sb solder alloy. Materials Science and Engineering A Vol. 448 (2007), pp. 287-293.

[4] Morozumi, A; Hokazono, H; Nishimura, Y.; Ikeda, Y.; Nabetani, Y.; Takahashi, Y: Direct Liquid Cooling Module with High Reliability Solder Joining Technology for Automotive Applications. 25th International Symposium on Power Semiconductor Devices & ICs (2013), pp. 109-112.

[5] Morelle, J.M.; Tan, K.L.; Vivet, L.; Leon, R.; Lavrentieff, S.; Geeds, V.: Alternative lead free die attach for power module packaging. CIPS 2012, paper 09.2.

[6] Nishiura, A.; Morozumi, A.: Evolved life of IGBT module suitable for electric propulsion system. PCIM Europe (2009), pp. 367-371.

[7] Adachi, S.; Nagaune, F.; Gohara, H.; Hitachi, T.; Morozumi, A.; Dietrich, P., Nishiura, A.: High thermal conductivity technology to realize high power IGBT modules for electric and hybrid vehicles. PCIM Europe (2012), pp. 1378-1384.

[8] Dugal, F.; Ciappa, M.: Avoiding misleading artefacts in metallurgical preparation of die attach solder joints in high power modules. Microelectronics Reliability Vol. 53-9-11 (2013), pp. 1403-1408.

[9] Lee, C.C.; Wang, P.J.; Kim, J.S.: Are Intermetallics in Solder Joints Really Brittle? 2007 Electronic Components and Technology Conference, pp. 648-6522.

[10] Geranmayeh, A.R.; Nayyeri, G.; Mahmudi, R.: Microstructure and impression creep behavior of lead-free Sn-5Sb solder alloy containing Bi and Ag.